Finite Element Modeling of Seismic Faulting With A Laboratory-Derived Rate And State Dependent Friction Law

H.L. Xing and A. Makinouchi

Materials Fabrication Lab, RIKEN, Hirosawa 2-1, Wako, Saitama, Japan
A. Makinouchi<akitake@postman.riken.go.jp>
H.L. Xing<xing@postman.riken.go.jp>

Abstract

Earthquakes have been recognized as resulting from a stick-slip frictional instability along the faults between deformable rocks. This paper introduces the recent development of our research activity in the finite element analysis of the static or quasi-static deformable rocks in contact along the faults with a laboratory-derived rate and state dependent friction law.

1. Introduction

The earthquakes can be regarded as a contact between deformable rocks with a special friction law along the faults (e.g. Marone C. 1998). An arbitrarily shaped contact element strategy, named as node-to-point contact element strategy, was proposed by the authors and applied to handle the friction contact(even the thermocontact)between deformable bodies with stick and finite frictional slip(Xing and Makinouchi et al, 1998 a b; 1999 a b). This paper will focus on how to extend our algorithm to simulate the active faults. As for the seismic wave propagation, it will be simulated by a dynamic code (Guo and Makinouchi *et al*, 1999).

2. Constitutive Equation for Friction Contact

Consider two deformable bodies B^1 and B^2 with surfaces $S^1$and S^2, respectively, to contact on an interface S_c, and $S_c = S^1 \cap S^2$, $S_c^\alpha = S_c \cap S^\alpha$, where superscript $\alpha = 1,2$ refers to body B^α (as show in Fig.1).

2.1 General case

(1). Normal contact stress
We choose the penalty method to treat the normal constraints when contact occurs. For a slave node,

$$f_n = E_n sign(g_n) g_n = -E_n g_n \tag{1}$$

here E_n is the penalty parameter to penalize the penetration (gap) in the normal direction, and $g_n = \boldsymbol{n} \cdot (\boldsymbol{x}_s - \boldsymbol{x}_c)$.

(2). Friction Stress
A standard Coulomb friction model, with an additional limit on the allowable shear stress, is applied in an analogous way to the flow plasticity rule. And an increment decomposition of the sticking and the slipping is used. Finally friction stress can be described as follows (Xing and Makinouchi et al 1998 a, b)(*Note:* A variable with ~ on top stands for a relative component between slave and master bodies, and *l, m=1,2* in this paper):

$$f_m = \eta_m \overline{F} \tag{2}$$

where $\overline{F}$ is the critical frictional stress, $\overline{F} = min(\mu f_n, F_{limit})$; F_{limit} is a allowable value of shear stress; μ is the friction coefficient, it may depends on the normal contact pressure f_n, the equivalent slip velocity $\dot{\tilde{u}}^{sl}_{eq}$, the state variable φ and the temperature T, *i.e.* $\mu = \mu(f_n, \dot{\tilde{u}}^{sl}_{eq}, \varphi, T)$. So, when $F_{limit} > \mu f_n$,

$$\overline{F} = \mu(f_n, \dot{\tilde{u}}^{sl}_{eq}, \varphi, T)\ f_n \tag{3}$$

and

$$\eta_m = f^e_m \Big/ \sqrt{f^e_l f^e_l}\ ; \quad f^e_m = E_t(\tilde{u}_m - \tilde{u}^p_m\big|_0) = E_t(\tilde{u}^e_m + \Delta\tilde{u}_m) \tag{4}$$

here $\tilde{u}^p_m\big|_0$ is the value of $\tilde{u}^p_m$ at the beginning of this step.

In a summary, the linearized form of the friction stress can rewritten as,

$$df_l = \frac{\overline{F}E_t}{\sqrt{f^e_l f^e_l}}(\delta_{lm} - \eta_l\eta_m)d\tilde{u}_m + \eta_l\mu\left(df_n + \frac{\partial\mu}{\partial f_n}df_n\right) + \eta_l f_n\left(\frac{\partial\mu}{\partial\dot{\tilde{u}}^{sl}_{eq}}d\dot{\tilde{u}}^{sl}_{eq} + \frac{\partial\mu}{\partial\varphi}d\varphi + \frac{\partial\mu}{\partial T}dT\right) \quad (\text{if } \overline{F} = \mu f_n)$$

$$df_l = \frac{\overline{F}E_t}{\sqrt{f^e_l f^e_l}}(\delta_{lm} - \eta_l\eta_m)d\tilde{u}_m + \eta_l\frac{\partial\overline{F}}{\partial T}dT \quad (\text{if } \overline{F} = F_{limit}) \tag{5}$$

2.2 Rate and State Dependent Friction Laws for Rocks without Temperature Effects

Experimental studies on the frictional sliding in rocks was done and interpreted by Dieterich (1978,1979) and Ruina(1983) have led to a somewhat more realistic constitutive description. The shear strength τ depends on normal stress σ_n, slip velocity V and on the prior slip history in the form of dependence on a set of phenomenological parameters called state variables φ_i which evolve with ongoing slip. Ruina(1983) stated that

$$\tau = \sigma_n\left(\mu_0 + \varphi + a\ \ln\left(V/V_{ref}\right)\right) \qquad d\varphi\ /dt = -\left[(V/L)\left(\varphi\ + b\ \ln\left(V/V_{ref}\right)\right)\right] \tag{6}$$

and for a steady state,

$$\tau^{ss} = \sigma_n\left[\mu_0 + (a-b)\ln\left(\mathrm{V}/\mathrm{V}_{\mathrm{ref}}\right)\right] \tag{7}$$

where $$a = V\left(\partial\tau/\partial V\right)_\varphi \Big/ \sigma_n = \left(\partial\tau/\partial\ln V\right)_\varphi \Big/ \sigma_n \qquad a-b = \left(d\tau^{ss}/d\ln V\right)\Big/\sigma_n \tag{8}$$

Here, a and b are empirically determined parameters; a represents the instantaneous rate sensitivity, while a-b characterizes the long-term rate sensitivity. Depending on whether a-b is positive or negative, the frictional response is either velocity strengthening or velocity weakening, respectively. L is the critical slip distance; V_{ref} and V are an arbitrary reference velocity and a sliding velocity; φ is the state variables; σ_n is the effective normal contact stress; μ_0 is the steady friction coefficient at reference velocity V_{ref}.

Replacing V with $\dot{\tilde{u}}^{sl}_{eq}$ in the above equations, the friction coefficient μ can be described in a 3-dimensional form as

$$\mu = \mu_0 + \varphi + a\ ln\left(\dot{\tilde{u}}^{sl}_{eq} / \dot{\tilde{u}}^{sl}_{ref}\right) \tag{9}$$

$$d\varphi\ /dt = -\left[(V/L)\left(\varphi\ + b\ ln\left(\dot{\tilde{u}}^{sl}_{eq} / \dot{\tilde{u}}^{sl}_{ref}\right)\right)\right] \tag{10}$$

From Eqs. (1), (6)-(11), the contact stress acting on a slave node can be described as

$$\dot{f}_i = G_{ij}\dot{\tilde{u}}_j \tag{11}$$

where $\boldsymbol{G}$ is the frictional contact matrix for the rate and state dependent friction law.

3. Finite Element Formulation

3.1 Variational principle

The updated Lagrangian rate formulation is employed to describe the finite deformation problem. The rate type equilibrium equation and the boundary at the current configuration are equivalently expressed by a principle of virtual velocity of the form

$$\int_V \{ (\sigma^J_{ij} - 2\sigma_{ik}D_{kj})\delta D_{ij} + \sigma_{jk}L_{ik}\delta L_{ij} \} dV = \int_{S_\Gamma} \dot{F}_i \delta v_i dS + \int_{S^1_c} \dot{f}^1_i \delta v_i dS + \int_{S^2_c} \dot{f}^2_i \delta v_i dS \tag{12}$$

where V and S denote respectively the domain occupied by the total body B and its boundary at time t; S_Γ is a part of the boundary of S on which the rate of traction $\dot{F}_i$ is prescribed; $\delta\boldsymbol{v}$ is the virtual velocity field which satisfies the boundary $\delta\boldsymbol{v} = \boldsymbol{0}$ on the velocity boundary; $\boldsymbol{L}$ is the velocity gradient tensor, $\boldsymbol{L} = \partial\boldsymbol{v}/\partial\boldsymbol{x}$; $\boldsymbol{D}$ and $\boldsymbol{W}$ are the symmetric and antisymmetric parts of $\boldsymbol{L}$, respectively.

The small strain linear elasticity and large strain rate-independent work-hardening plasticity are assumed to derive the elasto-plastic tangent constitutive tensor C^{ep}_{ijkl}:

$$\sigma^J_{ij} = C^{ep}_{ijkl}D_{kl} = C^{ep}_{ijkl}L_{kl} \tag{13}$$

Substitution of Eq.(13) into Eq.(12) reads to the final form of the virtual velocity principle:

$$\int_V \Sigma_{ijkl}\, L_{kl}\delta L_{ij} dV = \int_{S_\Gamma} \dot{F}_i \delta v_i dS + \int_{S^1_c} \dot{f}^1_i \delta v_i dS + \int_{S^2_c} \dot{f}^2_i \delta v_i dS \tag{14}$$

where $\Sigma_{ijkl} = C^{ep}_{ijkl} + (\sigma_{jl}\delta_{ik} - \sigma_{ik}\delta_{jl} - \sigma_{il}\delta_{jk} - \sigma_{jk}\delta_{il})/2$

3.2 Contact Force of A Slave Node on Master Segment

To calculate the contact force in Eq.(12), we assume that contact segment surfaces are described by $\boldsymbol{x} = \boldsymbol{x}(\xi_m)$, a slave node s has made contact with a master segment on point c (as shown in Fig. 2), and the contact force acting on it can be described in the local contact coordinate system as follows,

$$\begin{aligned} \dot{\boldsymbol{f}} &= \dot{f}_i\,\boldsymbol{e}_i + f_i E_{ijm}\,\boldsymbol{e}_j\,\dot{\xi}_m \\ &= \left(G_{ik}\,\boldsymbol{e}_i + C_{jk}\,\boldsymbol{e}_j\right)\dot{\tilde{u}}_k + f_i E_{ijm} D_m g^0_n\,\boldsymbol{e}_j / h \end{aligned} \tag{15}$$

Here $E_{ijm} = \boldsymbol{e}_{i,m}\cdot \boldsymbol{e}_j$, $\overline{C}_{ml} = C_{ml} - \boldsymbol{g}\cdot \boldsymbol{e}_{m,l} \doteq C_{ml} - g_n^0\, \boldsymbol{n}\cdot \boldsymbol{e}_{m,l}$, h is the determinant of $\overline{C}_{ml}$, g_n^0 is the penetration of last increment step; $D_m = \overline{C}_{ll}\, \dot{\boldsymbol{u}}_{c,m}\cdot \boldsymbol{n} - \overline{C}_{ml}\, \dot{\boldsymbol{u}}_{c,l}\cdot \boldsymbol{n}$; $\dot{\tilde{\boldsymbol{u}}} = \dot{\boldsymbol{u}}_s - \dot{\boldsymbol{u}}_c$, while $\dot{\boldsymbol{u}}_c$ is the velocity of material position c on the segment, $\dot{\boldsymbol{u}}_c = N_\gamma\, \dot{\boldsymbol{u}}_\gamma$, and $\dot{\boldsymbol{u}}_\gamma$ is the nodal velocity on the segment, where N_γ is the shape function of the segment; $\hat{\boldsymbol{e}}_k$ is the base vector of local Cartesian coordinate system on the contact interface. The reverse contact stress acting on a node γ of a master segment can be obtained as,

$$\dot{\boldsymbol{f}}_\gamma^2 = -N_\gamma\, \dot{\boldsymbol{f}} = -N_\gamma \left\{ \left(G_{ik}\, \boldsymbol{e}_i + C_{jk}\, \boldsymbol{e}_j \right) \dot{\tilde{u}}_k + f_i E_{ijm} D_m g_n^0\, \boldsymbol{e}_j / h \right\} \tag{16}$$

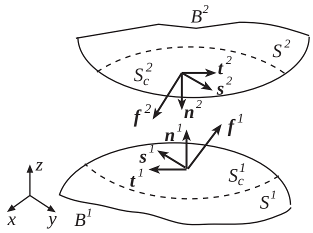

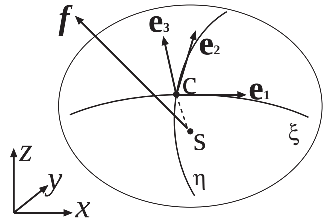

Fig. 1 Bodies in contact with each other   Fig.2 Frame for calculation of the contact force

3.4 Time integration algorithm

The time integration method is one of key issues to formulate an elasto-plastic finite element method. It is well known that the fully implicit method is often subjected to bad convergence problems, mostly due to changes of contact and friction states. In order to avoid this, we employ an explicit time integration procedure as follows. It is assumed that under a sufficiently small time increment all rates in Eq. (14) can be considered constant within the increment from t to $t + \Delta t$ as long as there is no drastic change of states (for example, elastic to plastic at an integration point, contact to discontact or discontact to contact on the contact interface, stick to slide or slide to stick in friction on the contact interface) takes place. The R-minimum method (Yamada, 1968) is extended and used here to limit the step size in order to avoid such drastic change in state within an incremental step.

Thus all the rate quantities used to derive Eq. (14) are simply replaced by incremental quantities as,

$$\Delta \boldsymbol{u} = \boldsymbol{v}\, \Delta t, \qquad \Delta \boldsymbol{\sigma} = \boldsymbol{\sigma}^J \Delta t, \qquad \Delta \boldsymbol{L} = \boldsymbol{L}\, \Delta t \tag{17}$$

Finally, in combination with Eqs. (15)-(17), Eq.(14) can be rewritten as

$$(\boldsymbol{K} + \boldsymbol{K}_f)\Delta \boldsymbol{u} = \Delta \boldsymbol{F} + \Delta \boldsymbol{F}_f \tag{18}$$

Here $\boldsymbol{K}$ is the standard stiffness matrix corresponding to body B; $\boldsymbol{K}_f$, stiffness matrix of the contact elements, comes from the contribution of the terms related with $\dot{\tilde{u}}_k$ in Eqs. (15) and (16); $\Delta \boldsymbol{u}$ is the nodal displacement increment; $\Delta \boldsymbol{F}$ is the external force increment subjected to body B on s_F; $\Delta \boldsymbol{F}_f$ comes from the contribution of the terms related with g_n^0 in Eqs. (15) and (16);

4. Applications

A direct shear 'sandwich' experimental model for friction studies is taken as an example to be investigated without state dependence. Due to the symmetry, only half of it is analyzed here (see

Fig. 3). At first, the body A is loaded along the x direction until $u_x = 0.138 \times 0.07$, then all the nodes on this loaded surface are fixed along x direction and the body B is moved along y direction. The stress distribution along the contact interface is not homogenous after the first stage (as shown in Fig.4). For the second stage, the relative displacement, the friction coefficient and the relative velocity at the different positions of the interface are quite different as shown in Fig.5, Fig.6 and Fig.7, respectively.

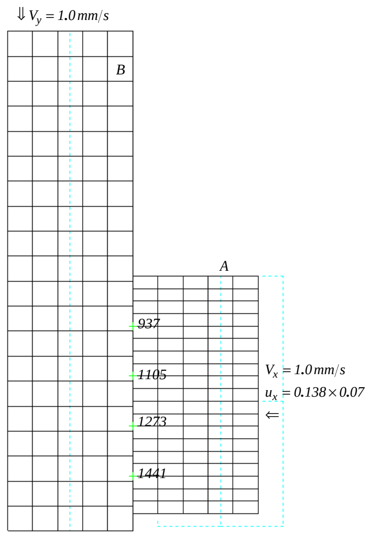

Fig. 3 The model analyzed

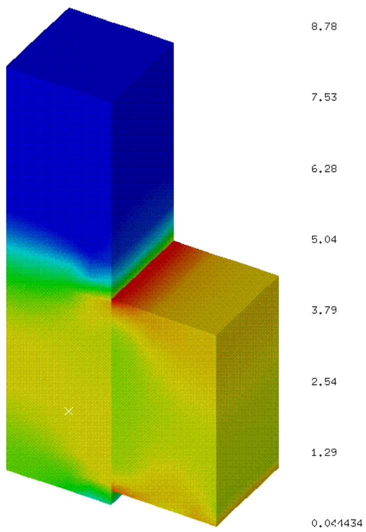

Fig.4 Mises stress distribution($u_x = 0.138 \times 0.07mm, u_y = 0$)

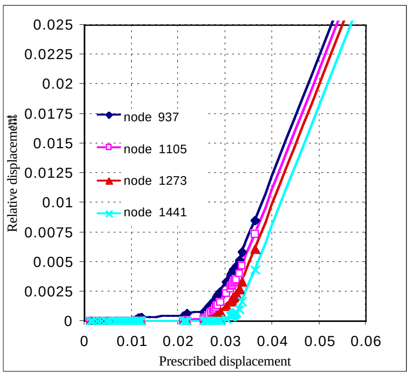

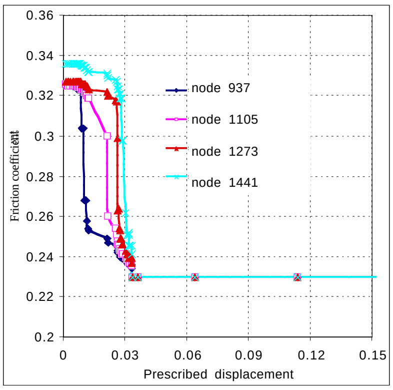

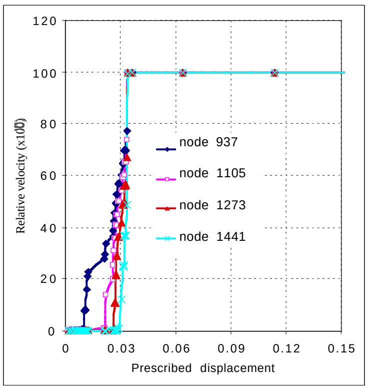

Fig.5 Relative displacement at different positions

Fig. 6 Friction coefficient at different positions

Fig.7 Relative velocity at different positions

5. Conclusions

The node-to-point contact element strategy proposed by authors based on the static-explicit algorithm was successfully extended to simulate the active faults with a rate and state dependent friction law. The applied example shows its stability, efficiency and usefulness. It is being applied to simulate the practical active faults around Japan.

6. References

Dieterich J H. 1978. Time-dependent friction and the mechanics of stick-slip. *Pure Appl. Geophys.* 116:790-806

Dieterich J H. 1979. Modeling of rock friction 1. Experimental results and constitutive equations, *J. Geophys. Res.* 84:2161-2168

Guo Z, Makinouchi A and Fujimoto T. 1999. FEM simulation of dynamic sliding of faults connecting static deformation process to dynamic process, *ACES Workshop Abstracts,* Australia, 213-220

Hirahara K. 1999. Quasi-static simulation of seismic cycle of great inter-plate earthquakes following a friction law in laterally heterogeneous viscoelastic medium under gravitation - FEM approach. *ACES Workshop Abstracts*, Australia. pp. 221-225.

Ruina A L. 1983. Slip instability and state variable friction laws, *J. Geophys. Res*. 88:10359-10370

Marone C. 1998. Laboratory-derived friction laws and their application to seismic faulting. *Annu. Rev. Earth Planet. Sci*. 26:643-696

Xing H L and Makinouchi A. 1998 a. FE modeling of 3-D multi-elasto-plastic-body contact in finite deformation, part 1. A node-to-point contact element strategy, part 2. Applications. *Proc. of JSCTP*, No.322&323, JSTP, 1998.5

Xing H L, Fujimoto T and Makinouchi A. 1998 b. Static-explicit FE modeling of 3-d large deformation multibody contact problems on parallel computer, *Proc. of NUMIFORM'98*, Ed Huetink, J & Baaijens, F P T. A.A. Balkema, 207-212

Xing H L, Fujimoto T and Makinouchi A. 1999 a. FE modeling of multiple thermal-elastic-plastic body contact in finite deformation and its application to tube and tubesheet assembling. *NAFEMS World Congress on Effective Engineering Analysis.* 669-682

Xing H L and Makinouchi A. 1999 b. Thermal-elastic-plastic FE modeling of frictional contact between finite deformation bodies. *Proceedings of the Conference on Computational Engineering and Science.* Vol. 4, pp. 629-632. 1999.5

Yamada Y, Yoshimura N and Sakurai T. 1968. Plastic stress-strain matrix and its application for the solution of elastic-plastic problems by finite element method, Int. J. Mech. Sci., 10: 343-354